Back to Session Subjects

THE APPLICATION OF AIR-JET VORTEX GENERATORS TO CONTROL THE FLOW ON HELICOPTER ROTOR BLADES

Neil P Lewington, David J Peake, Frank S Henry, Anastasios Kokkalis† and John Perry†

City University, London UK

Abstract

The usefulness of Air-Jet Vortex Generators (AJVGs) as a means of flow control to enhance rotor section performance has been conceptually explored under quasi-steady conditions in the wind tunnel. Utilising only small amounts of blowing ($C\mu \leq 0.01$, $Re_c = 1.1 \times 10^6$, $M_\infty = 0.1$), we demonstrate that stall can be delayed by up to 6°, lift increased by up to 25%, drag reduced by up to 50% and the lift/drag envelope extended accordingly.

Nomenclature

AJVG	air-jet vortex generator
b	aerofoil span
c	aerofoil chord
C_{Dp}	(CD), wake profile drag coefficient
C_N	normal force coefficient
C_P	pressure coefficient
C_{Pte}	trailing-edge pressure coefficient
C_μ	Blowing momentum coefficient $= \dot{m} V_J / 0.5 \rho U_\infty^2 c$
$\dot{m}$	AJVG mass flow rate
M	Mach number
Re_c	Reynolds number based on aerofoil chord
U_∞	freestream axial velocity
V_J	Jet resultant velocity
α	angle of attack
ϕ	angle of pitch of AJVG relative to aerofoil surface tangent
ψ	angle of skew of AJVG relative to freestream flow
ρ_∞	freestream fluid density

1. Introduction

Improved rotor aerodynamic performance continues to be a major area where helicopter vehicle performance improvements can be generated. Work continues to expand the operating envelope determined by the onset of stall and shock-induced separations on the aerofoil sections and tip planforms of rotor blades. Currently, improvements rely on conventional shape design techniques to achieve higher performance. To continue the improve rotor capability in the future, novel flow control techniques offer breakthroughs; but a much-improved understanding of the causes of flow breakdown is required, particularly under dynamic conditions.

Active flow control utilising low energy systems to fine tune the rotor blade top flow in both the spanwise and chordwise directions, coupled to a simpler rotor blade geometry (to reduce design and production costs) offers a way forward. The evaluation of an innovative concept at City University's Centre for Aeronautics to capitalise on this approach is demonstrated for a range of lifting systems up to transonic Mach numbers[1-9]. The concept involves employing low momentum air-jet vortex generators (AJVGs) to enhance the natural mixing in the shear layers above a rotor blade.

AJVGs consist of small jets emerging from an aerodynamic surface that are pitched and yawed relative to the oncoming freestream flow. The interaction between the air-jets and the freestream flow forms well-organised vortical structures with 'powered' cores that are capable of withstanding especially severe adverse pressure gradients as they penetrate downstream. The combined flow acts to suppress boundary layer separation and maintains the linearity of the lift curve to high incidence values. We postulate that by exploiting this aerodynamic technology and suitably configuring a helicopter rotor blade with an array of AJVGs, significant improvements in terms of lift enhancement will be gained in both the quasi-steady (medium-alpha) and unsteady (high-alpha) flow regimes. The simple installation geometry of AJVGs into a full-scale rotor blade top surface (taking account of the spanwise pumping available within the rotating blade potentially facilitates control of the entire viscous flow, from subsonic along the blade, to transonic at the tip. The design installation must be carefully considered remembering that it is desirable to keep rotor blades as uncomplicated and as inexpensive as possible, due to frequent life-cycle replacement.

† Formerly GKN-Westland

2. Experimental Arrangement

Aerofoil model

A NACA 23012 aerofoil with a modified trailing-edge geometry was chosen that is representative of the subcritical sections of a helicopter rotor blade (Figure 1). The aerofoil was specifically designed to incorporate trailing-edge separation in its flow field just prior to stall and, therefore, could benefit from both trailing-edge and leading-edge treatments. The aerofoil had been previously tested in the dynamic stall facility at the University of Glasgow at approximately the same Reynolds number and Mach number as the current test[10] and, therefore, its characteristics were well defined. The model was configured with two arrays of 15 AJVGs across the span, located at respective 12% and 62% chord positions. Each of the AJVG in the arrays configured so as to produce a co-rotating array of vortices, i.e., the rotational sense of the vortices generated across the rotor span are identical (Figure 2(b)). Static pressure measurements were made via 28 pressure tappings across the chord at three spanwise locations (0.375b, 0.5b and 0.75b), from which sectional normal force coefficients were determined. Transition was fixed by a strip of nominal 29μm roughness elements extending from the leading-edge to 0.03c on the aerofoil upper surface.

Wind tunnel

Experimental data were obtained in City University's T2 low speed wind tunnel, with the model unswept and mounted vertically in the working section. T2 is a closed circuit type wind tunnel consisting of a working section size of width 0.81m, height 1.12m and length 1.68m. Tests were conducted at a Reynolds number of 1.1×10^6 based on the chord of 486mm and freestream conditions for an incidence range of $-6° \le \alpha \le 20°$. Nominally two-dimensional flow across the aerofoil span was established throughout the incidence range by mounting the aerofoil between two endplates and employing tangential blowing to control the model/endplate junction boundary layer growth. Adequacy of nominal 2-D flow was verified from monitoring the parallelism of mini-tufts in the endplate/aerofoil junctions. Wake total pressure profile measurements were evaluated at the model centreline one chord length downstream of the aerofoil.

Air-jet vortex generators (AJVGs)

Installation of the AJVGs into the NACA 23012 aerofoil combined the spacing and geometry recommendations of Pearcey[1,3] and Freestone[2]. Each jet slot has a rectangular geometry with a slot aspect ratio of approximately 5 that is pitched at 30° and skewed at 60° relative to the oncoming flow (Figure 2(a)). Air is supplied to the AJVG arrays via two separate pressure regulated plenum chambers at x/c=0.12 and 0.62, operating at low blowing momentum coefficients, $0.005 < C_\mu < 0.01$.

Measurement accuracy

Validity of the experimental findings relies on the ability to minimise the intrinsic errors associated with data measurement. Although it is impossible to completely eradicate experimental errors, steps can be taken to minimise their influence on the results.

Two separate methods were utilised to measure the angle of attack (α) of the model in the wind tunnel relative to the tunnel centreline. The first uses a brass arc (radius 325mm) with an inscribed scale between 0° and 45° that is embedded into the wind tunnel floor. A scored line through the reference chord, over the entire length of the perspex endplate, could then be aligned with the brass arc to measure α to within ±0.125°. a second pointer was attached to the spindle about which the model was rotated. The pointer (radius 425mm) passed over a second scale permitting measurement of the incidence to within ±0.06°.

Measurements of the chordwise static pressure distribution and wake properties were made with pressure transducers connected to a CED 1401 data acquisition system. The accuracy of the pressure measurement is dependent upon the analogue to digital converters within the CED 1401. All voltage signals from the pressure transducers (within a ±5V range) are handled with 12 bit accuracy, i.e., ±2.4mV. At a tunnel speed of 35ms^{-1}, the dynamic head ($0.5\rho_\infty U_\infty^2$) equates to 830mV and hence a resolution in excess of ±0.29% could be achieved in the value of C_P.

3. Results and discussion

The chordwise static pressure distributions at the model centreline for three angles of attack with the AJVGs off (C_μ=0) are depicted on Figure 3. Note that when the aerofoil is in the unblown configuration, the air-jet slots are open; but there is no flow through the plenum chambers within the aerofoil. At α=10°, the flow remains attached at the aerofoil trailing-edge, but there is evidence of a separation bubble on the upper surface of the aerofoil close to the leading-edge. The separation bubble persists at α=15° and a region of separated flow is apparent at the trailing-edge of the aerofoil emanating from approximately 0.80c. By α=18°, the flow has separated over the majority of the upper

surface of the aerofoil. Stall is indicated when C_{Pte} goes from a positive value to a negative value and diverges.

Figure 4 shows the spanwise variation of the chordwise static pressure distributions (measured at 0.375b, 0.5b and 0.75b) on the aerofoil at α=15° with the AJVGs inactive. With the exception of the extreme leading-edge position where suction is at a maximum, due to the high curvature on the aerofoil, the pressure distributions are nearly identical indicating that the flow has a high degree of two-dimensionality, despite the presence of significant separation near the trailing-edge. Further evidence of the spanwise uniformity of the flow is demonstrated by the trailing-edge pressure coefficient variation with angle of attack plot, Figure 7. Little variation is apparent in the data to well beyond the onset of flow separation from the trailing-edge.

The effectiveness of controlling both leading-edge and trailing-edge stalling by employing the AJVGs is shown in Figures 5-9. Figure 5 shows that AJVGs can largely restore attached flow at the high angle of incidence of 18°, although rear AJVGs alone cannot reattach flow at this incidence. Note that the total jet momentum blowing coefficient is very low ($C_\mu \leq 0.01$) for all these cases. Blowing at 0.12c and 0.12c + 0.62c together lessens the extent of the separated flow region promoting near full pressure recovery at the aerofoil trailing-edge.

The elevated surface pressure distributions perpendicular to the chord (C_P vs y/c), shown on Figure 6, are indicative of the enhancement in nose suction that results from blowing at 0.12c and 0.12c + 0.62c. The AJVGs restore a velocity around the aerofoil leading-edge commensurate with conditions of attached flow rather than largely separated flow at this α=18° without flow control.

By defining the onset of flow separation as being the point at which C_{Pte} goes negative, Figure 7 shows that it is possible to delay the onset of separation by up to 4° when blowing from 0.62c; and up to 6° when blowing from 0.12c and 0.12c + 0.62c ($C_\mu \leq 0.01$ in all cases). Multi-symbology on the plot indicates measurements taken at the three spanwise pressure tapping locations. Blowing from the trailing-edge is not as powerful as from the leading-edge but still offers significant improvement and may be more attractive for rotor blade application, since it does not interfere with the structural spar, the erosion shield or the de-icing arrangements of typical rotor blades.

Figure 8 highlights the improvements on the normal force coefficient (C_N), profile drag coefficient (C_{Dp}) and quarter chord pitching moment coefficient ($C_{M1/4c}$) with angle of attack. In each case employing the AJVGs results in an increase in the measured C_{Nmax} and a delay in the drag divergence. Blowing from the array at 0.62c increases C_{Nmax} by 15% whilst blowing at 0.12c and 0.12c + 0.62c yields respective C_{Nmax} increases of 21% and 25%.

The effect of blowing momentum coefficient ($C_\mu \leq 0.01$ at x/c=0.12) on the incremental normal force on the aerofoil at constant angle of attack, is demonstrated on Figure 9. The range of C_μ shown is small ($C_\mu < 0.01$). A near linear relationship is exhibited for dC_N/dC_μ 'steepening' with increasing angle of attack. At α=18°, the curve asymptotes towards a ΔC_N of 0.4 for $C_\mu > 0.005$. The effect is mainly to restore the unseparated flow values of C_N and $C_{M1/4c}$. If C_μ continues to increase, the curves asymptote to the same low rate of increase seen at α=10° suggesting that there are two mechanisms at work: separation control and circulation enhancement. The circulation enhancement is small because the jet orifices are small, inclined to the surface and located near to the leading-edge.

Figure 10 shows the influence of employing the AJVGs on the momentum deficit in the wake at the wind tunnel centreline one chord length downstream of the aerofoil at α=16°. With the AJVGs off, the aerofoil is stalled and has a very wide wake. Employing air-jets at either chordwise location results in a significant reduction in the wake width. The upper half of Figure 11 shows that the maximum C_N/C_{Dp} is significantly enhanced and that the enhancement occurs at the highest values of C_N. The figure also shows that blowing from the rear position is more adept at improving the aerofoil lift/drag efficiency.

The lower half of Figure 11 shows the drag polar itself. It can be seen that blowing from the rear location is very effective at delaying drag divergence. Blowing from the leading-edge can extend the low drag range but the drag values for the trailing-edge blowing location are significantly lower prior to drag divergence. Note that blowing has little effect on drag prior to the onset of separation on the unblown configuration.

4. Conclusions

We have demonstrated that installing two co-rotating arrays of air-jet vortex generators on a modified NACA 23012 yields considerable enhancement of the aerofoil performance characteristics. Operating with a low momentum

blowing coefficient ($C_\mu \leq 0.01$) from the AJVG arrays at 0.12c + 0.62c together yields the following key results. Sectional C_{Nmax} is increased by 25% above the uncontrolled case, the trailing-edge static pressure divergence is delayed by up to 6°and there is a major extension of the C_N/C_{Dp} envelope, essentially due to the prevention of separation onset.

References

1) H H Pearcey, "Shock induced separation and its prevention by design and boundary layer control", 'Boundary layer and flow separation control', Pergamon Press, pp1166-1344, 1961

2) M M Freestone, "Preliminary tests at low speed on vorticity produced by air-jet vortex generators", RM 85/1, Centre for Aeronautics, City University, 1985

3) H H Pearcey, K Rao and D M Sykes, "Inclined air-jets used as vortex generators to suppress shock induced boundary layer separation", AGARD-CP-534, Paper 40, 1993

4) F S Henry and H H Pearcey, "Numerical model of boundary layer control using air-jet generated vortices", AIAA Journal, Vol 32, No. 12, pp2415-2425, 1994

5) F Innes, H H Pearcey and D M Sykes, "Improvement in the performance of a three element high lift system by the application of airjet vortex generators", Proc CEAS European Forum, 'High Lift and Separation Control', Royal Aeronautical Society, pp25.1-25.11, London 1995

6) S D Akanni and F S Henry, "Numerical modelling of air jet vortex generators in turbulent boundary layers", Proc CEAS European Forum, 'High Lift and Separation Control', Royal Aeronautical Society, pp16.1-16.12, London 1995

7) A G Oliver, "Air jet vortex generators for wind turbines", PhD thesis, Centre for Aeronautics, City University, Dec 1997

8) C Küpper, "A study of the application of air-jet vortex generators to intake ducts", PhD thesis, Centre for Aeronautics, City University, July 1999

9) D J Peake, F S Henry and H H Pearcey, "Viscous flow control with air-jet vortex generators", Paper No. AIAA 99-3175, 17th AIAA Applied Aerodynamics Conference, Norfolk, Virginia, 28 June - 1 July 1999

10) M W Gracey, "The design and low Mach number wind-tunnel performance of a modified NACA 23012 aerofoil, with an investigation of dynamic stall", PhD Thesis 8916, University of Glasgow, 1991

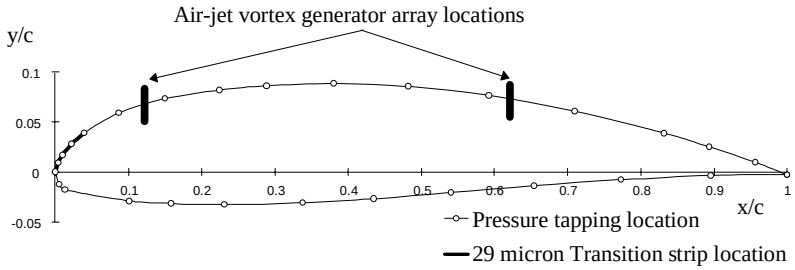

Figure 1: Chordwise profile of the modified NACA 23012 aerofoil

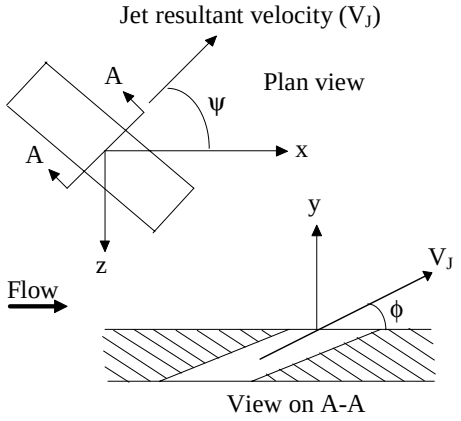

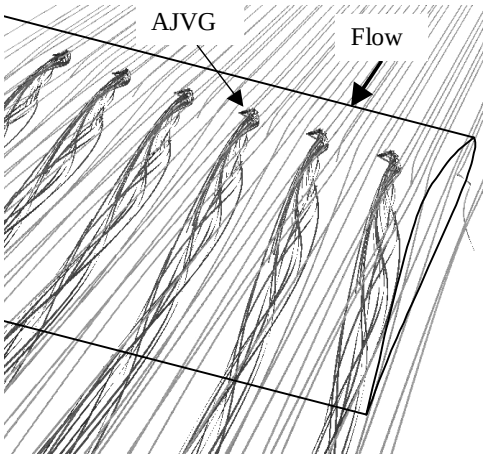

Figure 2: (a) Air jet slot configuration (b) AJVG installation on a rotor blade

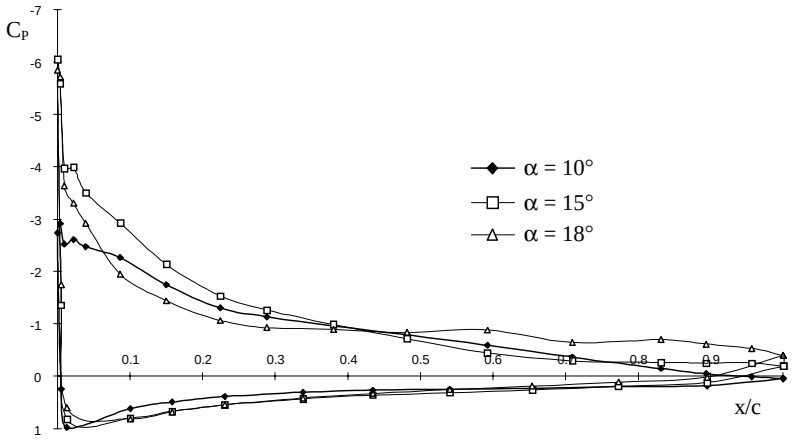

Figure 3: Sensitivity of chordwise surface pressure distributions to incidence, at centre span, with $C_\mu=0$, $Re_c=1.1\times10^6$

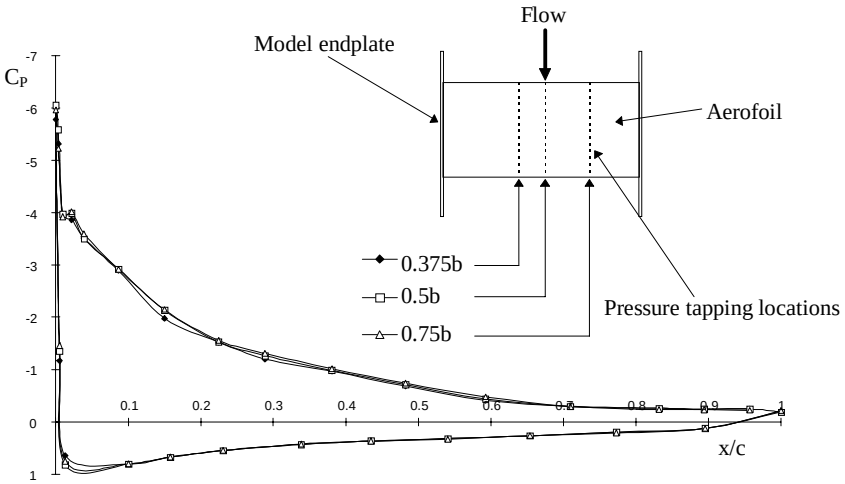

Figure 4: Spanwise variation of the chordwise surface pressure distribution at α=15°, C_μ=0, Re_c=1.1×10^6

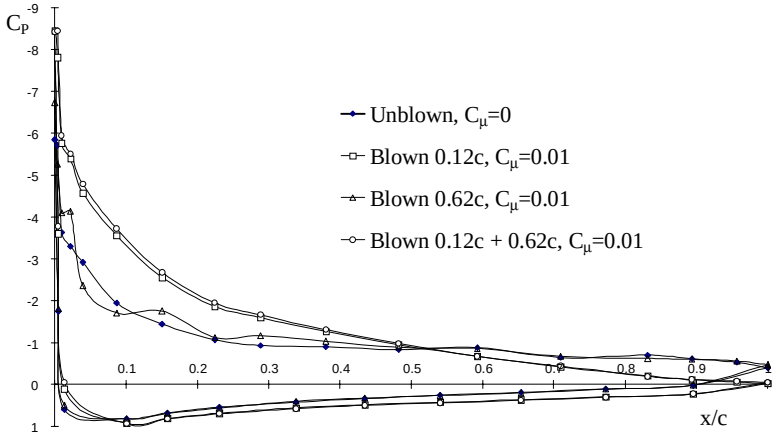

Figure 5: Sensitivity of chordwise surface pressure distributions at tunnel centreline to AJVG chordwise array position at α=18°, Re_c=1.1×10^6, ϕ=30°, ψ=60°

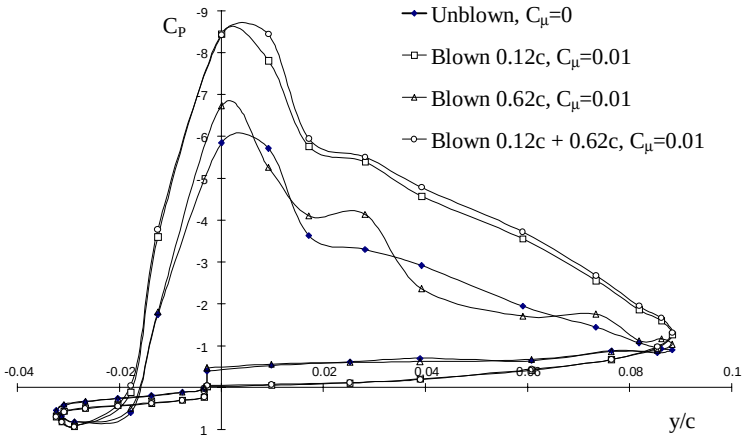

Figure 6: Sensitivity of thickness surface pressure distributions at tunnel centreline to AJVG array chordwise position at α=18°, Re_c=1.1×10^6, ϕ=30°, ψ=60°

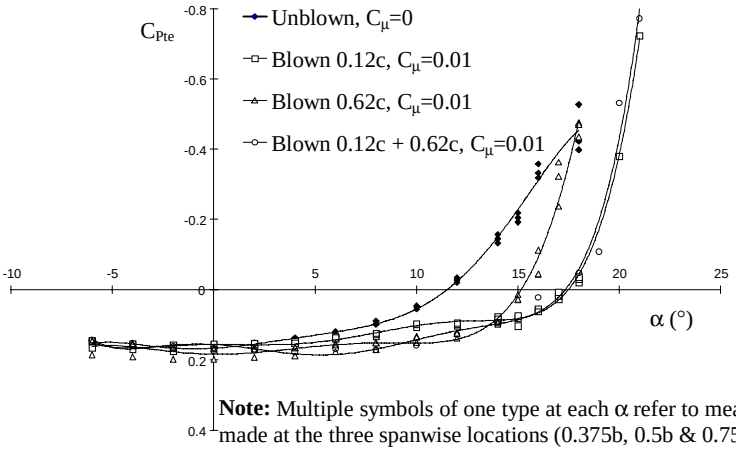

Figure 7: Trailing edge pressure coefficient variation with angle of attack, $Re_c=1.1\times10^6$, $\phi=30°$, $\psi=60°$

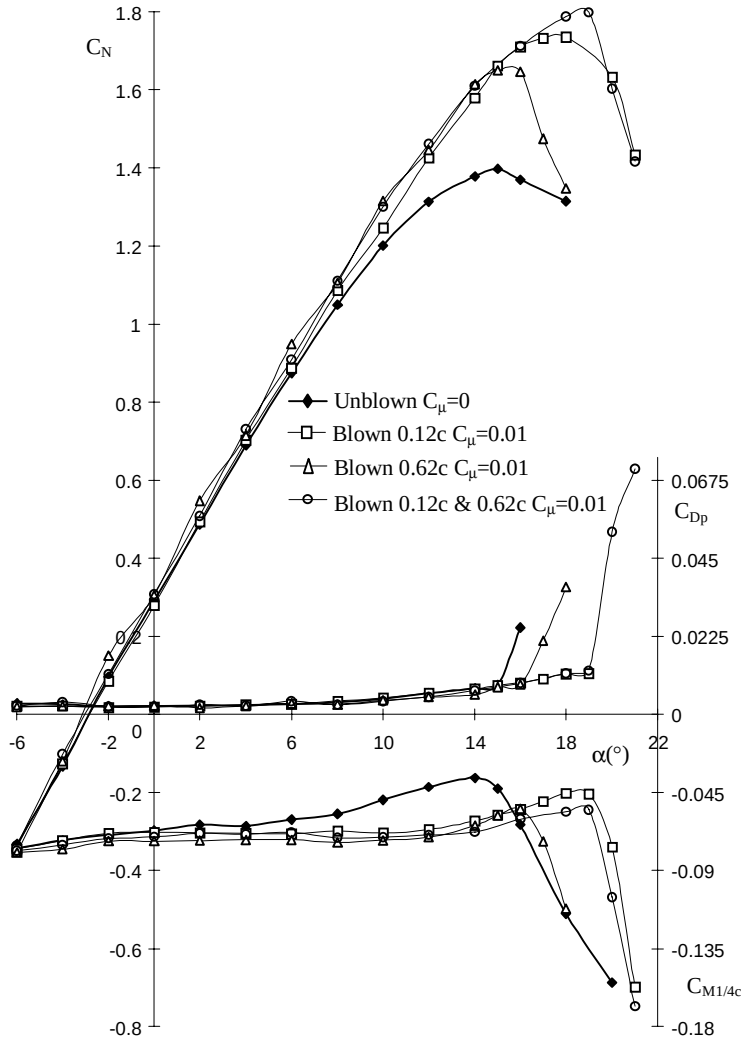

Figure 8: Normal force, wake profile drag and quarter chord pitching moment variation with angle of attack, $Re_c=1.1\times10^6$, $\phi=30°$, $\psi=60°$

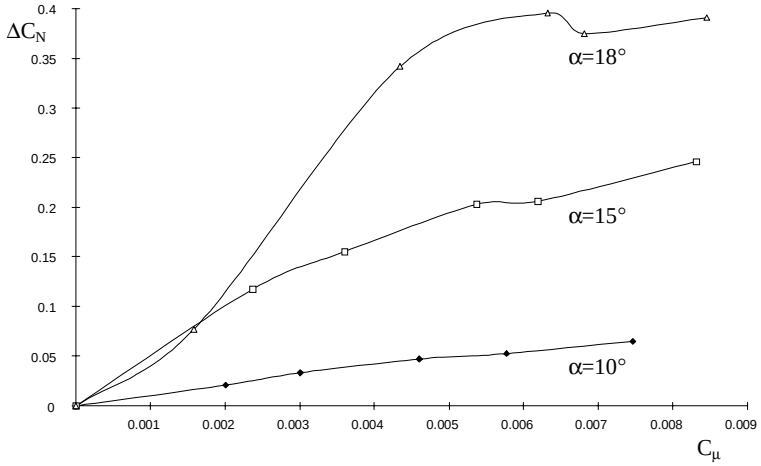

Figure 9: Normal force increment with blowing momentum coefficient (Blowing at x/c=0.12c), $Re_c=1.1\times10^6$, $\phi=30°$, $\psi=60°$

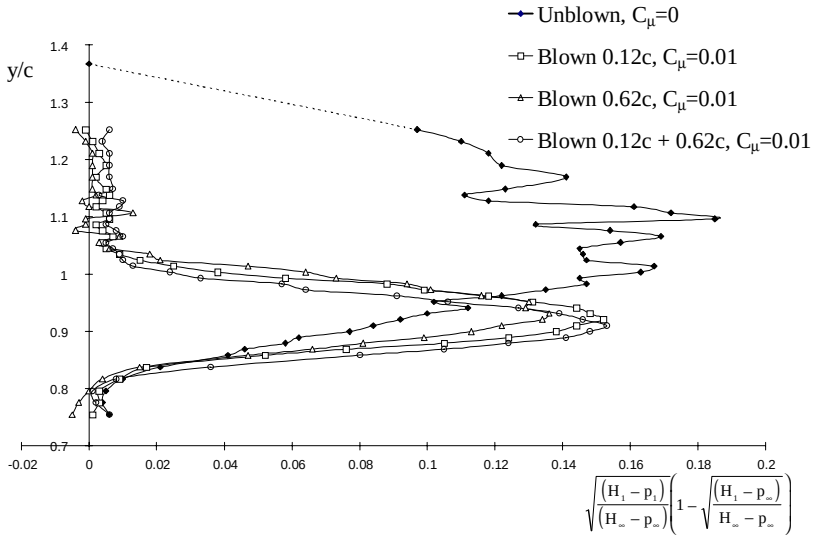

Figure 10: Wake profiles measured one chord length downstream of the modified NACA 23012 aerofoil at $\alpha=16°$, $Re_c=1.1\times10^6$, $\phi=30°$, $\psi=60°$

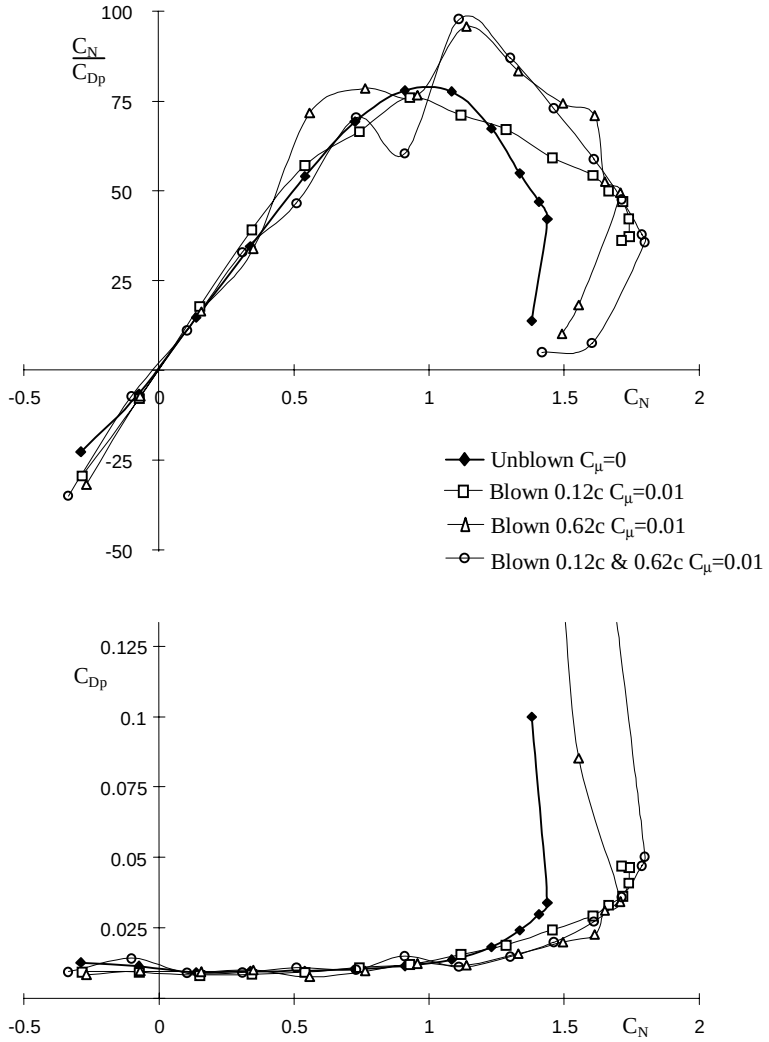

Figure 11: Normal force/drag and wake profile drag polars, $Re_c=1.1\times10^6$, $\phi=30°$, $\psi=60°$

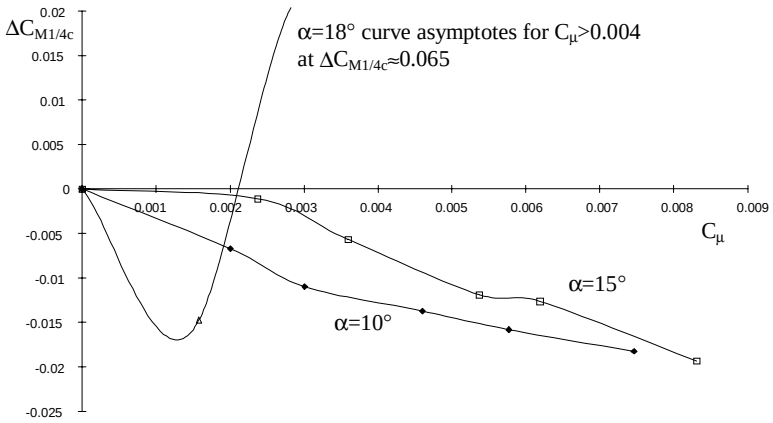

Figure 12: Variation of incremental quarter chord pitching moment with blowing momentum coefficient (Blowing at x/c=0.12c), $Re_c=1.1\times10^6$, $\phi=30°$, $\psi=60°$